Title
Cyclodextrin metalâorganic framework-based protein biocomposites

Permalink
https://escholarship.org/uc/item/75k8p61n

Authors
Di Palma, Giuseppe
Geels, Shannon
Carpenter, Brooke P
et al.

Publication Date
2022

DOI
10.1039/D2BM01240E

Data Availability
The data associated with this publication are available upon request.

Peer reviewed

ARTICLE

Cyclodextrin metal-organic framework-based protein biocomposites

Giuseppe Di Palma,[a] Shannon Geels,[b,c] Brooke P. Carpenter,[a] Rain A. Talosig,[a] Charles Chen,[a] Francesco Marangoni,[b,c] Joseph P. Patterson[†a,d]

Materials are needed to increase the stability and half-life of therapeutic proteins during delivery. These materials should be biocompatible and biodegradable. Here, we demonstrate that enzymes and immunoproteins can be encapsulated inside cyclodextrin based metal-organic frameworks using potassium as the metal node. The release profile can be controlled with the solubility of the cyclodextrin linker. The activity of the proteins after release is determined using catalytic and in vitro assays. The results show that cyclodextrin metal-organic framework-based protein biocomposites are a promising class of materials to deliver therapeutic proteins.

Introduction

Metal-Organic Framework-based protein biocomposites (p@MOFs) are extended crystalline materials where the protein is encapsulated within the ordered lattice of metal nodes and organic linkers.[1–3] This material is in contrast to protein-metal-organic frameworks where the biomolecule is a part of the lattice.[4,5] P@MOFs present an exciting opportunity for next-generation materials in biosensing[6], drug delivery[7–9], imaging,[10,11] and cancer therapy[12–16] due to the increased stability and activity of the encapsulated proteins.[17–19] In general, MOFs have been widely studied as drug delivery materials due to their high drug loading,[20] and controllable drug release properties.[21–23] A key factor when designing MOFs for drug delivery is the toxicity of the individual metal and ligand components.[24,25] In 2010, Stoddard and coworkers created an "edible" MOF using gamma-cyclodextrin (γ-CD) and potassium or rubidium to form CD-MOF1 and CD-MOF2, respectively.[26] More recently CD-MOFs have been formed using α-CD[27] and β-CD[28]. These CD-MOFs have been investigated for applications in gas sensing[29], enantiomeric separation[30], catalysis,[31] and small molecule drug delivery.[32] CD-MOFs are especially attractive for drug delivery systems as they display low toxicity compared to other MOF linkers.[33] CD-MOFs should be ideal for the storage and delivery of therapeutic proteins as cyclodextrin-protein complexes display sustained drug delivery,[34,35] reduced protein

aggregation, and higher structural stability to physical perturbation.[36] In addition, cyclodextrins can induce the refolding of denatured proteins.[37]

Furthermore, the importance of proteins being integrated with sugars is already represented in nature, where carbohydrates are incorporated into >50% of human proteins.[38] For this reason there has been great interest in the development of new carbohydrate based drug delivery systems.[39–41] However, to the best of our knowledge, biomolecule encapsulation inside CD-MOFs has not been demonstrated.[32,42] The reason for this is likely because the original synthesis for CD-MOF1 requires a high pH environment (~13) and extended crystallization times (~several days);[42] the combination of which would likely denature proteins. Another challenge when developing CD-MOFs for drug delivery is controlling their release profile.[43] Here, we develop a quick (several hours) and biofriendly (pH ~8.5) synthesis for CD-MOF1 and β-CD-MOF using potassium as the metal node. Protein encapsulation is demonstrated using bovine serum albumin (BSA), catalase, myoglobin, and interleukin-2. We further developed a method to manufacture CD-MOF pellets that results in sustained release over 24 hours.
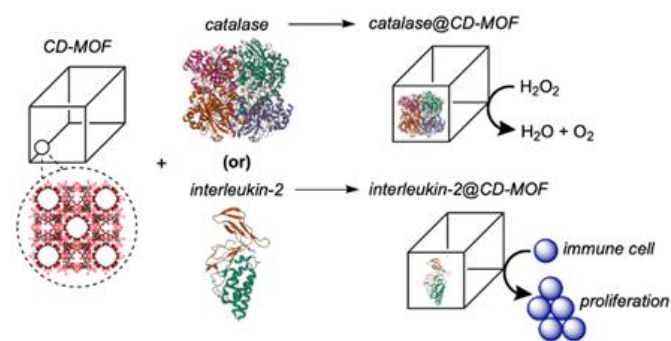
Scheme 1. Encapsulation of proteins (Catalase/Interleukin-2) and the activity of the related CD-MOF biocomposites, as catalyst for oxygen removal, and as immunomodulator for immune cell proliferation

a. Department of Chemistry, University of California Irvine, Irvine, California 92697, United States.
b. Department of Physiology and Biophysics, University of California Irvine, Irvine, CA 92697, USA
c. Institute for Immunology, University of California Irvine, Irvine, CA 92697, USA.
d. Department of Materials Science and Engineering, University of California Irvine, Irvine, California 92697, United States
† Corresponding author e-mail: patters3@uci.edu

The activity of catalase and interleukin-2 after release is demonstrated using catalytic and in vitro assays respectively.

Results and discussions

CD-MOFs were synthesized by dissolving the precursors in pure water and inducing crystallization through the addition of a non-solvent. Methanol or acetonitrile were used as the non-solvent for γ- and β-CD-MOFs respectively. Encapsulation efficiency (EE%) for the protein@CD-MOFs was determined using the Bradford assay, which found the EE% for all proteins studied to be ~80-98% (Figure 1, Table S1.). During the last step of the synthesis, the CD-MOFs are centrifuged, separated from supernatant, and dried under a constant airflow inside 2 ml centrifugation tubes to form a compact pellet of approximately 1 cm in diameter (Figure 2g, 3g). Powder X-Ray Diffraction (PXRD) of the γ-CD-MOFs and protein@γ-CD-MOFs showed peaks consistent with literature (Figure 2a),[26,44] with a maximum d-spacing of ~2.2 nm (SI Table S2). SEM images of BSA, myoglobin, and catalase γ-CD-MOFs showed truncated cuboid crystals (Figure 2 c, d, e). SEM images of interleukin-2@γ-CD-MOFs showed rough spheroid crystals (Figure 2 f).
PXRD of the protein-β-CD-MOFs showed peaks consistent with literature,[44] and a maximum d-spacing of ~2.0 nm (Figure 3a, Table S2). It is important to note that the XRD patterns are consistent regardless of the biomolecule used. This consistency occurs because proteins are entrapped into defects of the crystal lattice rather than altering the crystal lattice. [17,45–48] SEM

images of β-CD-MOFs and BSA@β-CD-MOFs show cuboid crystals; SEM images of catalase and interleukin-2 β-CD-MOFs showed rhomboid crystals; and myoglobin β-CD-MOFs showed rough spheroid structures (Figure 3 b-f). The collective SEM data reveals that incorporation of biomolecules into the CD-MOF synthesis effects the nucleation and growth mechanism resulting in different crystal morphologies, consistent with previous protein@MOFs studies.[17,49] The solid pellets (Figure 2g and 3g) were considered optimal for a release profile study without further post-synthesis modification. The release profile was obtained for the BSA@ γ-CD-MOFs, BSA@ β-CD-MOFs, and
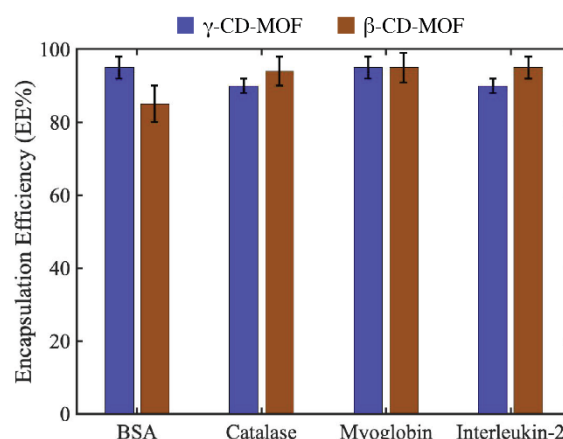

Fig. 1 Encapsulation Efficiency of BSA, Catalase, Myoglobin, and Interleukin-2 for γ-CD-MOFs (blue) and β-CD-MOFs (brown). Error determined by triplicates
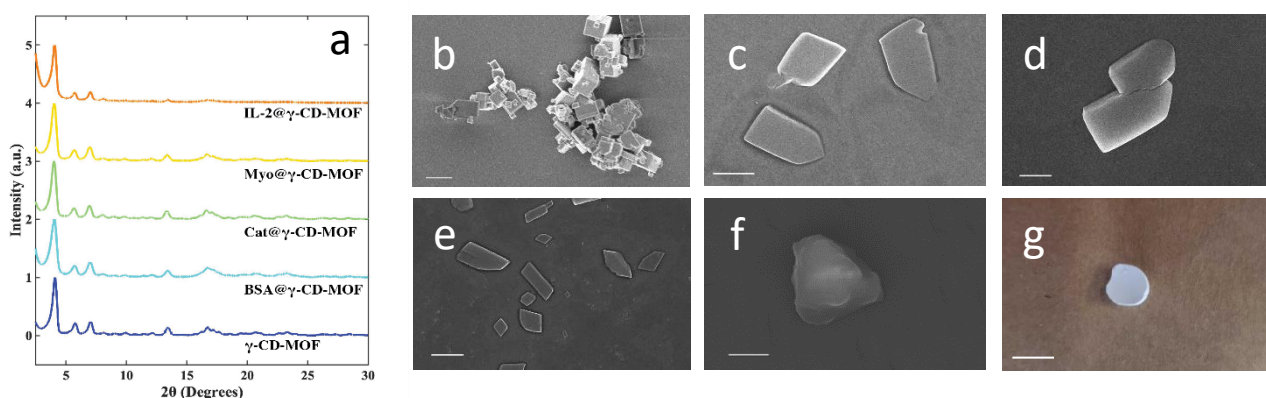

Fig.2 a) PXRD of γ-CD-MOFs and SEM of b) γ-CD-MOFs c) BSA@γ-CD-MOFs d) Catalase@γ-CD-MOFs e) Myoglobin@γ-CD-MOFs f) Interleukin-2@γ-CD-MOFs. Scale bar: 2 μm. g) pellet of protein@γ-CD-MOFs. Scale bar:1 cm
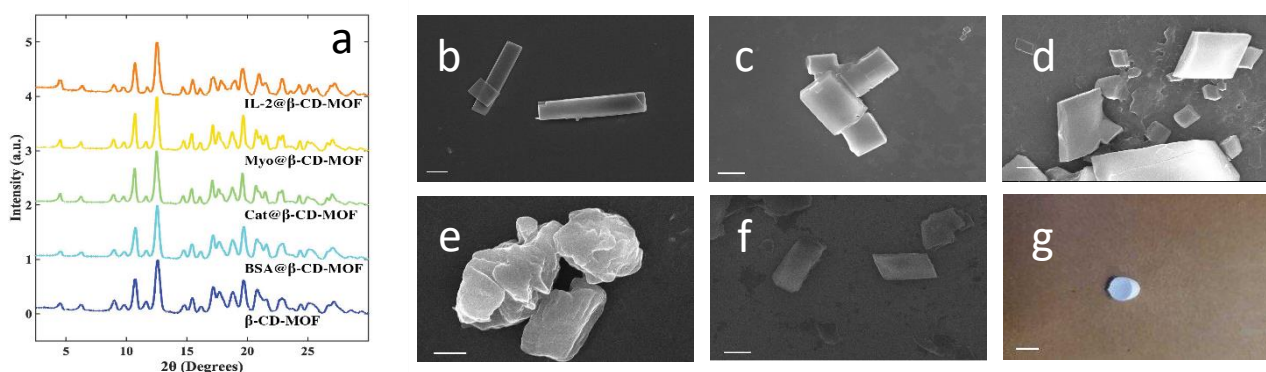

Fig.3 a) PXRD of β-CD-MOFs and SEMs of b) β-CD-MOFs c) BSA@β-CD-MOFs d) Catalase@β-CD-MOF e) Myoglobin@β-CD-MOFs f) Interleukin-2@β-CD-MOFs. Scale bar : 2 μm g) pellet of protein@β-CD-MOFs. Scale Bar: 1 cm.

a hybrid of BSA@ γ-/β-CD-MOFs (γ : β 1:1) system (Figure 4). The hybrid BSA@ γ-/β-CD-MOF was designed to examine the tunability of the protein release profile. SEM images of the hybrid of γ-/β-CD-MOF showed a mixture of γ-/β-CD-MOF crystals and aggregates with irregular shapes (SI figure S1-S2). PXRD of the hybrid CD-MOF showed a low crystallinity compared to the CD-MOFs with only one type of organic linker. This indicates that mixing with more than one type of cyclodextrin could interfere with the extensivity of the crystal lattice. γ-CD-MOFs displayed the fastest release with full release being achieved within 10 minutes. β-CD-MOF displayed the slowest release profile with full release being achieved over ~24 hours. We hypothesize that the lower solubility of β-CD in water compared to γ-CD is the main factor between the difference in release profile.[50] The hybrid γ-/β-CD-MOF pellet displayed an intermediate release profile indicating that the release profile can be tuned. Since it was possible to tune the release profile using the hybrid CD-MOF, we believe that the release profile is determined by the solvation of the outermost organic linkers. When solvated, the crystal structure breaks down which then liberates the encapsulated protein. To evaluate the protein@CD-MOFs as delivery systems, we tested the activity of the catalase@CD-MOFs and interleukin-2@CD-MOFs after dissolution. The activity of catalase@CD-MOFs was evaluated by comparing the catalytic activity with free catalase using the FOX assay (figure 5).[51] The data shows that after release, the catalase from the γ-CD-MOFs shows no activity; however, the catalase from the β-CD-MOFs has comparable activity to the free catalase. We hypothesize that the difference in activity is due to methanol weakening the hydrophobic interactions that form the tertiary structure of a protein. This deterioration of tertiary structure results in a loss of activity in the enzyme.[52,53] We measured the biological activity of encapsulated interleukin-2 using an in vitro T cell proliferation assay. We loaded primary mouse T cells with CellTrace Violet, a fluorescent dye that distributes equally to the daughter cells upon proliferation. Thus, non-proliferating cells show a single peak of high fluorescence as measured by flow cytometry, while

proliferating cells display peaks of progressively lower fluorescence, each corresponding to the number of cell divisions. Unstimulated T cells and cells cultured in presence of
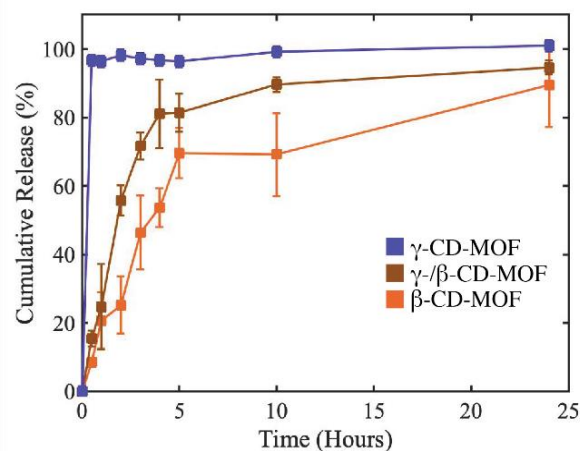

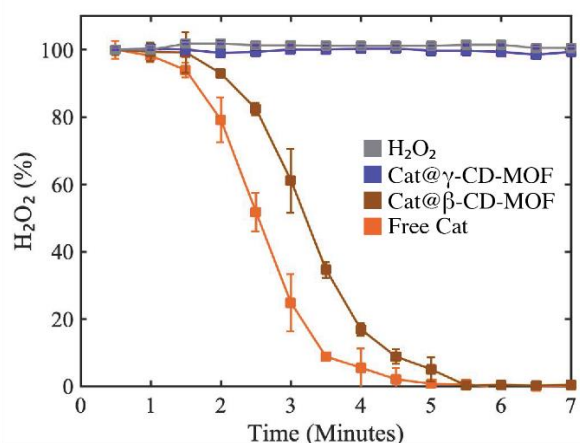Fig.4 Release profiles of BSA encapsulated in β-CD-MOFs (blue), γ-/β-CD-MOFs (brown), and γ-CD-MOFs (orange).

Fig.5 Catalytic assay of free Catalase (orange), Catalase encapsulated into β-CD-MOF (brown), Catalase encapsulated into γ-CD-MOF (blue), and no catalase (gray). Stirring at 300 rpm was used in all solutions during the experiment.
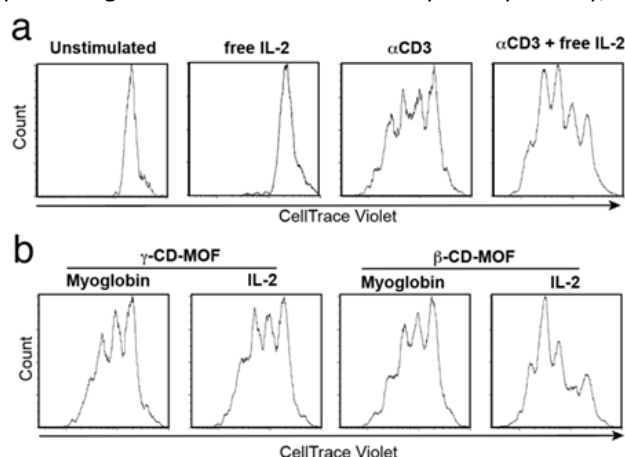

Figure 6. a. CellTrace Violet fluorescence profiles of CD4+ T cells either unstimulated or cultured with 200 ng/ml free interleukin-2 (IL-2), 50 ng/ml anti-CD3ε antibodies, or anti-CD3ε + 20 ng/ml free interleukin-2. b. CellTrace Violet profiles of CD4+ T cells stimulated with anti-CD3ε + myoglobin or interleukin-2 encapsulated to γ or β-CD-MOF (20 ng/ml). c. Proliferation of CD4+ and CD8+ T cells after stimulation with anti-CD3ε plus graded doses of encapsulated myoglobin or interleukin 2, or free interleukin 2. Means and SD are shown. For encapsulated interleukin-2, * signifies $p<0.05$ towards the correspondent encapsulated myoglobin, while # symbolizes $p<0.05$ against free interleukin-2. Statistical analysis by Student's t test. One experiment representative of two is shown.
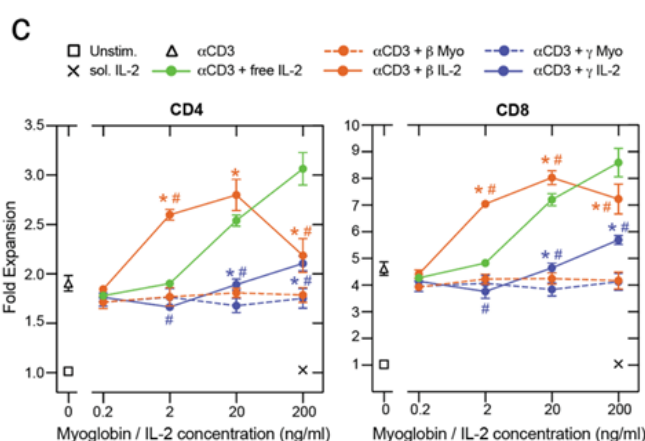
free interleukin-2 did not proliferate. T cells stimulated using antibodies recognizing CD3ε, a molecule associated to the T cell receptor, showed basal levels of proliferation that were greatly enhanced by the addition of free interleukin-2 (Figure 6A). While interleukin-2@γ-CD-MOF failed to increase proliferation induced by anti-CD3ε antibodies compared to myoglobin@γ-CD-MOF, interleukin-2@β-CD-MOF greatly expanded T cells compared to myoglobin@β-CD-MOF (Figure 6B). We quantified T cell proliferation by calculating their fold expansion, the ratio between the number of cells at the end of the culture to the number of cells at the beginning of it. Increasing amounts of free interleukin-2 resulted in a dose-dependent rise of proliferation in CD4+ and CD8+ cells, the two main T cell subtypes (Figure 6C). Interleukin-2@γ-CD-MOF increased CD4 and CD8 T cell proliferation compared to myoglobin@γ-CD-MOF only at the doses of 20 and 200 ng/ml, and always to levels much lower than these achieved by free interleukin-2. On the other hand, interleukin-2@β-CD-MOF not only increased the proliferation of CD4 and CD8 T cells compared to myoglobin@β-CD-MOF at the doses of 2, 20 and 200 ng/ml, but also outperformed free interleukin 2 at the doses of 2 and 20 ng/ml (Figure 6C). The decrease in cell proliferation observed at 200 ng/ml of interleukin-2@β-CD-MOF may be explained by the shutoff of endogenous interleukin-2 production in cultured T cells, which occurs when high concentrations of interleukin-2 are added to the culture medium[54]. Because interleukin-2 is quickly internalized and degraded after binding to its receptor[55], interleukin-2 is progressively depleted from T cell cultures in vitro. The slow release of interleukin-2 from β-CD-MOF may thus prolong its availability to T cells over time and explain the higher biological activity of interleukin-2@β-CD-MOF compared to free interleukin-2.

Conclusions

In summary, we demonstrated the synthesis of cyclodextrin metal-organic framework-based protein biocomposites. Using different type of cyclodextrins, we have shown that the release profile can be tuned and the encapsulated proteins remain active after release from these materials. Encapsulation of catalase and interleukin-2 in γ-CD-MOF decreases their biological activity, while encapsulation in β-CD-MOF preserves it. We hypothesize that, during the synthesis of γ-CD-MOFs, methanol interferes and weakens hydrophobic interactions of the tertiary protein structures. Future p@CD-MOFs synthesis will focus on non-protic solvents as non-solvent for crystallization. These results demonstrate the importance of developing a biofriendly method for encapsulating biomolecules within MOFs. Considering that during release, the proteins will be in a cyclodextrin rich environment, we believe these materials are promising for the delivery of therapeutic proteins.

Conflicts of interest

There are no conflicts to declare

Acknowledgements

References

1   W. Liang, P. Wied, F. Carraro, C. J. Sumby, B. Nidetzky, C.-K. Tsung, P. Falcaro and C. J. Doonan, *Chem Rev*, 2021, **121**, 1077–1129.

2   C. Doonan, R. Riccò, K. Liang, D. Bradshaw and P. Falcaro, *Acc. Chem. Res.*, 2017, **50**, 1423–1432.

3   D. Zou, L. Yu, Q. Sun, Y. Hui, Tengjisi, Y. Liu, G. Yang, D. Wibowo and C.-X. Zhao, *Colloids and Surfaces B: Biointerfaces*, 2020, **193**, 111108.

4   J. B. Bailey and F. A. Tezcan, *J. Am. Chem. Soc.*, 2020, **142**, 17265–17270.

5   P. A. Sontz, J. B. Bailey, S. Ahn and F. A. Tezcan, *J. Am. Chem. Soc.*, 2015, **137**, 11598–11601.

6   M. Mohammad, A. Razmjou, K. Liang, M. Asadnia and V. Chen, *ACS applied materials & interfaces*, , DOI:10.1021/acsami.8b16837.

7   T.-T. Chen, J.-T. Yi, Y.-Y. Zhao and X. Chu, *J. Am. Chem. Soc.*, 2018, **140**, 9912–9920.

8   T. Simon-Yarza, A. Mielcarek, P. Couvreur and C. Serre, *Advanced Materials*, 2018, **30**, 1707365.

9   J. Cases Díaz, B. Lozano-Torres and M. Giménez-Marqués, *Chem. Mater.*, 2022, **34**, 7817–7827.

10 J. Zhang, M. He, C. Nie, M. He, Q. Pan, C. Liu, Y. Hu, J. Yi, T. Chen and X. Chu, *Anal. Chem.*, 2019, **91**, 9049–9057.

11 P. Horcajada, T. Chalati, C. Serre, B. Gillet, C. Sebrie, T. Baati, J. F. Eubank, D. Heurtaux, P. Clayette, C. Kreuz, J.-S. Chang, Y. K. Hwang, V. Marsaud, P.-N. Bories, L. Cynober, S. Gil, G. Férey, P. Couvreur and R. Gref, *Nature Mater*, 2010, **9**, 172–178.

12 Q. Zhao, Z. Gong, Z. Li, J. Wang, J. Zhang, Z. Zhao, P. Zhang, S. Zheng, R. J. Miron, Q. Yuan and Y. Zhang, *Advanced Materials*, 2021, **33**, 2100616.

13 K. Ni, T. Luo, G. T. Nash and W. Lin, *Acc. Chem. Res.*, 2020, **53**, 1739–1748.

14 K. Lu, C. He, N. Guo, C. Chan, K. Ni, R. R. Weichselbaum and W. Lin, *J. Am. Chem. Soc.*, 2016, **138**, 12502–12510.

15 Q. Li, Y. Liu, Y. Zhang and W. Jiang, *Journal of Controlled Release*, 2022, **347**, 183–198.

16 S. Jin, L. Weng, Z. Li, Z. Yang, L. Zhu, J. Shi, W. Tang, W. Ma, H. Zong and W. Jiang, *J. Mater. Chem. B*, 2020, **8**, 4620–4626.

17 K. Liang, R. Ricco, C. M. Doherty, M. J. Styles, S. Bell, N. Kirby, S. Mudie, D. Haylock, A. J. Hill, C. J. Doonan and P. Falcaro, *Nat Commun*, 2015, **6**, 7240.

18 T.-H. Wei, S.-H. Wu, Y.-D. Huang, W.-S. Lo, B. P. Williams, S.-Y. Chen, H.-C. Yang, Y.-S. Hsu, Z.-Y. Lin, X.-H. Chen, P.-E. Kuo, L.-Y. Chou, C.-K. Tsung and F.-K. Shieh, *Nat Commun*, 2019, **10**, 5002.

19 M. B. Majewski, A. J. Howarth, P. Li, M. R. Wasielewski, J. T. Hupp and O. K. Farha, *CrystEngComm*, 2017, **19**, 4082–4091.

20 S. Wuttke, M. Lismont, A. Escudero, B. Rungtaweevoranit and W. J. Parak, *Biomaterials*, 2017, **123**, 172–183.

21 M. Sindoro, N. Yanai, A.-Y. Jee and S. Granick, *Acc. Chem. Res.*, 2014, **47**, 459–469.

22 P. Horcajada, R. Gref, T. Baati, P. K. Allan, G. Maurin, P. Couvreur, G. Férey, R. E. Morris and C. Serre, *Chem. Rev.*, 2012, **112**, 1232–1268.

23 W. Cai, H. Gao, C. Chu, X. Wang, J. Wang, P. Zhang, G. Lin, W. Li, G. Liu and X. Chen, *ACS Appl. Mater. Interfaces*, 2017, **9**, 2040–2051.

24 C. Tamames-Tabar, D. Cunha, E. Imbuluzqueta, F. Ragon, C. Serre, M. J. Blanco-Prieto and P. Horcajada, *J. Mater. Chem. B*, 2013, **2**, 262–271.

25 R. Ettlinger, U. Lächelt, R. Gref, P. Horcajada, T. Lammers, C. Serre, P. Couvreur, R. E. Morris and S. Wuttke, *Chem. Soc. Rev.*, 2022, **51**, 464–484.

26 R. A. Smaldone, R. S. Forgan, H. Furukawa, J. J. Gassensmith, A. M. Z. Slawin, O. M. Yaghi and J. F. Stoddart, *Angewandte Chemie International Edition*, 2010, **49**, 8630–8634.

27 J. Sha, X. Yang, L. Sun, X. Zhang, S. Li, J. Li and N. Sheng, *Polyhedron*, 2017, **127**, 396–402.

28 J. Liu, T.-Y. Bao, X.-Y. Yang, P.-P. Zhu, L.-H. Wu, J.-Q. Sha, L. Zhang, L.-Z. Dong, X.-L. Cao and Y.-Q. Lan, *Chem. Commun.*, 2017, **53**, 7804–7807.

29 J. J. Gassensmith, J. Y. Kim, J. M. Holcroft, O. K. Farha, J. F. Stoddart, J. T. Hupp and N. C. Jeong, *J. Am. Chem. Soc.*, 2014, **136**, 8277–8282.

30 W. Xu, X. Li, L. Wang, S. Li, S. Chu, J. Wang, Y. Li, J. Hou, Q. Luo and J. Liu, *Frontiers in Chemistry*.

31 S. Han, Y. Wei and B. A. Grzybowski, *Chemistry – A European Journal*, 2013, **19**, 11194–11198.

32 I. Roy and J. F. Stoddart, *Acc. Chem. Res.*, 2021, **54**, 1440–1453.

33 M. P. Abuçafy, B. L. Caetano, B. G. Chiari-Andréo, B. Fonseca-Santos, A. M. do Santos, M. Chorilli and L. A. Chiavacci, *European Journal of Pharmaceutics and Biopharmaceutics*, 2018, **127**, 112–119.

34 M. Sivasubramanian, T. Thambi and J. H. Park, *Carbohydrate Polymers*, 2013, **97**, 643–649.

35 K. Chen, S. He, H. Wang, S. Zhang, L. Yu, Y. Zhang, E. H. Elshazly, L. Ke and R. Gong, *Journal of Polymer Engineering*, 2020, **40**, 440–447.

36 T. M. Goszczyński, M. Gawłowski, B. Girek, K. Kowalski, J. Boratyński and T. Girek, *J Incl Phenom Macrocycl Chem*, 2017, **87**, 341–348.

37 L. Zhang, Q. Zhang and C. Wang, *Biomedical Chromatography*, 2013, **27**, 365–370.

38 H. J. An, J. W. Froehlich and C. B. Lebrilla, *Curr Opin Chem Biol*, 2009, **13**, 421–426.

39 X. Di, X. Liang, C. Shen, Y. Pei, B. Wu and Z. He, *Pharmaceutics*, 2022, **14**, 739.

40 K. Liu, X. Jiang and P. Hunziker, *Nanoscale*, 2016, **8**, 16091–16156.

41 M. Fathi, Á. Martín and D. J. McClements, *Trends in Food Science & Technology*, 2014, **39**, 18–39.

42 T. Rajkumar, D. Kukkar, K.-H. Kim, J. R. Sohn and A. Deep, *Journal of Industrial and Engineering Chemistry*, 2019, **72**, 50–66.

43 H. Li, N. Lv, X. Li, B. Liu, J. Feng, X. Ren, T. Guo, D. Chen, J. F. Stoddart, R. Gref and J. Zhang, *Nanoscale*, 2017, **9**, 7454–7463.

44 Y. Xiong, L. Wu, T. Guo, C. Wang, W. Wu, Y. Tang, T. Xiong, Y. Zhou, W. Zhu and J. Zhang, *AAPS PharmSciTech*, 2019, **20**, 224.

45 Y. Jia, B. Wei, R. Duan, Y. Zhang, B. Wang, A. Hakeem, N. Liu, X. Ou, S. Xu, Z. Chen, X. Lou and F. Xia, *Sci Rep*, 2014, **4**, 5929.

46 S. Wang, Y. Chen, S. Wang, P. Li, C. A. Mirkin and O. K. Farha, *J. Am. Chem. Soc.*, 2019, **141**, 2215–2219.

47 Y. Chen, P. Li, J. A. Modica, R. J. Drout and O. K. Farha, *J. Am. Chem. Soc.*, 2018, **140**, 5678–5681.

48 Y. Sun, L. Zheng, Y. Yang, X. Qian, T. Fu, X. Li, Z. Yang, H. Yan, C. Cui and W. Tan, *Nano-Micro Lett.*, 2020, **12**, 103.

49 A. F. Ogata, A. M. Rakowski, B. P. Carpenter, D. A. Fishman, J. G. Merham, P. J. Hurst and J. P. Patterson, *J. Am. Chem. Soc.*, 2020, **142**, 1433–1442.

50 A. Semalty, *Expert Opinion on Drug Delivery*, 2014, **11**, 1255–1272.

51 W. Liang, H. Xu, F. Carraro, N. K. Maddigan, Q. Li, S. G. Bell, D. M. Huang, A. Tarzia, M. B. Solomon, H.

Amenitsch, L. Vaccari, C. J. Sumby, P. Falcaro and C. J. Doonan, *J. Am. Chem. Soc.*, 2019, **141**, 2348–2355.

52 Q. Shao, Y. Fan, L. Yang and Y. Qin Gao, *J. Chem. Phys.*, 2012, **136**, 115101.

53 A. Fernández and O. Sinanoglu, *Biophys Chem*, 1985, **21**, 163–166.

54 A. V. Villarino, C. M. Tato, J. S. Stumhofer, Z. Yao, Y. K. Cui, L. Hennighausen, J. J. O'Shea and C. A. Hunter, *J Exp Med*, 2007, **204**, 65–71.

55 A. Yu, F. Olosz, C. Y. Choi and T. R. Malek, *Journal of Immunology*, 2000, **165**, 2556–2562.